

1
2 **1 The role of defoliation and root rot pathogen infection in**
3
4 **2 driving the mode of drought-related physiological decline in**
5
6 **3 Scots pine (*Pinus sylvestris* L.)**

7
8
9
10
11
12 **4**
13
14
15
16 **5**
17
18
19 **6** D. AGUADÉ^{1,2,5}, R. POYATOS¹, M. GÓMEZ³, J. OLIVA⁴ and J. MARTÍNEZ-
20
21 **7** VILALTA^{1,2}

22
23
24 **8** ¹CREAF, Cerdanyola del Vallès E-08193 (Barcelona), Spain

25
26
27 **9** ²Univ. Autònoma Barcelona, Cerdanyola del Vallès E-08193 (Barcelona),
28
29 **10** Spain

30
31
32 **11** ³ Forest Science Centre of Catalonia, Solsona, Catalonia, Spain

33
34
35 **12** ⁴ Department of Forest Mycology and Plant Pathology, Uppsala Biocenter,
36
37 **13** Swedish University of Agricultural Sciences, Box 7026, S-750 07 Uppsala,
38
39 **14** Sweden

40
41
42 **15** ⁵Corresponding author: d.aguade@creaf.uab.es

43
44
45
46 **17** **Keywords:** die-off, fungi pathogen, global change, hydraulic failure, non-structural
47
48 **18** carbohydrates

49
50 **19**

51
52 **20**

1 2 21 Abstract

3
4 22 Drought-related tree die-off episodes have been observed in all vegetated continents.

5
6 23 Despite much research effort, however, the multiple interactions between carbon
7 24 starvation, hydraulic failure and biotic agents in driving tree mortality under field
8 25 conditions are still not well understood.

9
10 26 We analysed the seasonal variability of non-structural carbohydrates (NSC) in four
11 27 organs (leaves, branches, trunk and roots), the vulnerability to embolism in roots and
12 28 branches, native embolism (PLC) in branches and the presence of root rot pathogens in
13 29 defoliated and non-defoliated individuals in a declining Scots pine (*Pinus sylvestris* L.)
14 30 population in the NE Iberian Peninsula in 2012, which included a particularly dry and
15 31 warm summer.

16
17 32 No differences were observed between defoliated and non-defoliated pines in hydraulic
18 33 parameters, except for a higher vulnerability to embolism at pressures below -2 MPa in
19 34 roots of defoliated pines. No differences were found between defoliation classes in
20 35 branch PLC.

21
22 36 Total NSC (TNSC, soluble sugars plus starch) values decreased during drought,
23 37 particularly in leaves. Defoliation reduced TNSC levels across tree organs, especially
24 38 just before (June) and during (August) drought.

25
26 39 Root rot infection by the fungal pathogen *Onnia* spp. was detected but it did not appear
27 40 to be associated to tree defoliation. However, *Onnia* infection was associated with
28 41 reduced leaf specific hydraulic conductivity (K_L) and sapwood depth, and thus
29 42 contributed to hydraulic impairment, especially in defoliated pines. Infection was also
30 43 associated with virtually depleted root starch reserves during and after drought in
31 44 defoliated pines. Moreover, defoliated and infected trees tended to show lower Basal
32 45 Area Increment (BAI).

1
2
3 46 Overall, our results show the intertwined nature of physiological mechanisms leading to
4
5 47 drought-induced mortality and the inherent difficulty of isolating their contribution
6
7 48 under field conditions.
8
9
10 49

11 50 **Introduction**
12
13
14

15 51 Drought-induced tree die-off is emerging as a global phenomenon, affecting a great
16
17 52 variety of species and ecosystems in all vegetated continents of the world (Allen et al.
18
19 53 2010). Recent episodes of crown defoliation and tree mortality have been related to an
20
21 54 increase of mean annual temperature and a decrease of annual rainfall in southern
22
23 55 European forests (Carnicer et al. 2011) and with increasing severe droughts in the
24
25 56 southwestern United States (Van Mantgem et al. 2009, Williams et al. 2012). Extreme
26
27 57 drought events are expected to become more frequent (IPCC 2013), which could
28
29 58 accelerate drought-related tree mortality. These responses can be amplified in many
30
31 59 regions by current trends towards increased stand basal area, associated with changes in
32
33 60 forest management (Martínez-Vilalta et al. 2012). There are important feedback loops
34
35 61 between forest dynamics and climate due to the key role of forests on the global water
36
37 62 and carbon cycles (Bonan 2008) and thus widespread forest mortality can have rapid
38
39 63 and drastic consequences for ecosystems (Anderegg et al. 2013a). Nonetheless, and
40
41 64 despite these potential effects on ecosystem functioning, the mechanisms causing tree
42
43 65 die-off are still poorly understood (Sala et al. 2010, McDowell 2011, McDowell et al.
44
45 66 2011).

46
47 67 McDowell et al. (2008) introduced a framework with three main, non-exclusive
48
49 68 mechanisms that could cause drought-induced mortality in trees: 1) carbon starvation, 2)
50
51 69 hydraulic failure and 3) biotic agents. They also hypothesized that plants with a strict
52
53 70 control of water loss through stomatal closure (isohydric species) would be more likely

1
2
3 71 to die of carbon starvation during a long drought, whereas anisohydric species would
4
5 72 more likely experience hydraulic failure during intense droughts, due to more negative
6
7 73 xylem water potentials (McDowell et al. 2008). However, the evidence for or against
8
9 74 these proposed mortality mechanisms is inconclusive, and recent reports have urged
10
11 75 adoption of a more integrated approach focusing on the interrelations between plant
12
13 76 hydraulics and the economy and transport of carbon in plants (McDowell and Sevanto
14
15 77 2010, Sala et al. 2010, McDowell 2011, McDowell et al. 2011, Sala et al. 2012).
16
17
18 78
19
20
21 79 Xylem vulnerability to embolism has been found to place a definitive limit on the
22
23 80 physical tolerance of conifers (Brodribb and Cochard 2009) and angiosperms (Urli et al.
24
25 81 2013) to desiccation. A recent global synthesis has shown that many tree species
26
27 82 operate within relatively narrow hydraulic safety margins in all major biomes of the
28
29 83 world (Choat et al. 2012). Although structural and physiological acclimation to drought
30
31 84 may result in large safety margins from hydraulic failure preceding death (Plaut et al.
32
33 85 2012), high levels of hydraulic dysfunction associated with drought-induced desiccation
34
35 86 have been reported (Hoffmann et al. 2011, Nardini et al. 2013). In addition, evidence of
36
37 87 hydraulic failure linked to canopy and root mortality has been found in declining
38
39 88 trembling aspen (*Populus tremuloides* Michx.), without evidence of depletion of
40
41 89 carbohydrate reserves (Anderegg et al. 2012), and in some *Eucalyptus* species (Mitchell
42
43 90 et al. 2013).
44
45
46
47
48 91 The dynamics and role of non-structural carbohydrate (NSC) stores during drought are
49
50 92 still under debate but some agreement is emerging in that NSC concentrations tend to
51
52 93 increase under moderate drought because growth ceases before photosynthesis, whereas
53
54 94 they may decline sharply if drought conditions become extreme (McDowell 2011).
55
56 95 Recent reports show that the same drought conditions can have contrasting effects on
57
58
59
60

1
2
3 NSC concentrations even on species of the same genus (*Nothofagus*) (Piper 2011). On
4
5 the other hand, Galiano et al. (2011) reported extremely low NSC concentrations in the
6
7 stem of defoliated Scots pine (*Pinus sylvestris* L.) trees and higher probability of
8
9 drought-induced mortality in pines with lower NSC concentrations. Also, Adams et al.
10
11 (2013) observed an association between tree mortality and reduced NSC levels in leaves
12
13 in a drought simulation experiment on piñon pine (*Pinus edulis* Engelm.). In addition,
14
15 drought-related reductions in stored NSC pools may affect tree organs differentially.
16
17 For instance, Hartmann et al. (2013a) showed a reduction of NSC in Norway spruce
18
19 (*Picea abies* (L.) Karst.) roots but not in leaves, which could be attributed to changes in
20
21 carbon allocation.
22
23

24
25 Biotic agents and drought can interact to accelerate tree mortality. Drought-stressed
26
27 trees may be more vulnerable to infection by fungal pathogens (Desprez-Loustau et al.
28
29 2006, La Porta et al. 2008) or to insect attacks (Matthias et al. 2007, Gaylord et al.
30
31 2013). Although pathogens can directly kill trees through the production of toxic
32
33 metabolites, they can also induce hydraulic failure, e.g. via occlusion of the xylem, or
34
35 carbon starvation by altering NSC demand or supply. The interactions between
36
37 pathogen infection and the physiological mechanisms of drought-induced mortality
38
39 depend on the trophic interaction (biotrophic, necrotrophic or vascular wilts) established
40
41 with the tree (Oliva et al. 2014). For instance, blue-stain fungi infection can cause
42
43 outright hydraulic failure via xylem occlusion (Hubbard et al. 2013) while root rot fungi
44
45 may lead to a gradual tree decline and eventually to death because of chronic growth
46
47 reductions and subsequent constraints on water transport (Oliva et al. 2012). In addition,
48
49 root rot fungi can reduce carbon reserves by fungal consumption of stored
50
51 carbohydrates or by the induction of carbon-expensive defences, causing tree growth
52
53 reductions (Cruickshank et al. 2011).
54
55
56
57
58
59
60

1
2
3 121 Field studies on mature trees examining all three hypothesized mechanisms of drought-
4
5 induced mortality are still scarce and rarely explore explicitly the interactions between
6
7 different mechanisms and their occurrence in different plant organs. Here we compare
8
9 124 the hydraulic properties and the dynamics of NSC and embolism as a function of
10
11 defoliation and infection by fungal pathogens in Scots pine trees growing together in a
12
13 site affected by drought-induced decline (Martínez-Vilalta and Piñol 2002, Heres et al.
14
15 2012) and close to the dry limit of the distribution of the species. Previous studies have
16
17 shown that defoliation precedes drought-induced mortality in Scots pine trees from the
18
19 same or similar sites (Galiano et al. 2011, Poyatos et al. 2013), and that defoliation
20
21 seems to be an inevitable consequence of drought in the most susceptible individuals
22
23 rather than an (effective) strategy to cope with it (Poyatos et al. 2013). In this context,
24
25 we address the following questions: 1) are defoliated Scots pines intrinsically more
26
27 vulnerable to xylem embolism than non-defoliated ones, providing evidence in favour
28
29 of hydraulic failure as an important component of the decline process? and, if so, do
30
31 defoliated trees experience higher levels of native embolism under dry summer
32
33 conditions? (i.e., are leaf area reductions enough to compensate for their intrinsically
34
35 higher vulnerability?); 2) do defoliated pines have lower seasonal NSC concentrations
36
37 in all organs, supporting carbon starvation being involved in the mortality process?; and
38
39 3) is infection by fungal pathogens likely to enhance hydraulic dysfunction through
40
41 increased levels of native embolism, or carbon depletion directly or indirectly lowering
42
43 NSC levels through increased consumption, reduced sapwood depth or low growth?.

44
45
46
47
48
49
50 142 **Materials and methods**
51
52
53
54
55
56
57
58
59
60

59 143 *Study site*

1
2
3 144 The study was conducted in Tillar valley (41° 19' N, 1° 00' E; 990 m a.s.l.) within
4
5 Poblet Forest Natural Reserve (Prades Mountains, NE Iberian Peninsula). The climate is
6
7 typically Mediterranean, with a mean annual precipitation of 664 mm (spring and
8
9 autumn being the雨iest seasons and with a marked summer dry period), and
10
11 moderately warm temperatures (11.3 °C on average) (Poyatos et al. 2013). The soils are
12
13 mostly Xerocrepts with fractured schist and clay loam texture, although outcrops of
14
15 granitic sandy soils are also present (Hereter et al. 1999). Our experimental area is
16
17 mostly located on a NW-facing hillside with a very shallow and unstable soil due to the
18
19 high stoniness and steep slopes (35° on average). More detailed information about the
20
21 study area can be found in Hereter and Sánchez (1999).

22
23
24 154 The dominant canopy tree species in the study site is Scots pine and the understory
25
26 consists mainly of the Mediterranean evergreen holm oak (*Quercus ilex* L.). Severe
27
28 droughts have affected the study site since the 1990's (Martínez-Vilalta and Piñol 2002,
29
30 Hereş et al. 2012). Scots pine average standing mortality and crown defoliation in the
31
32 Tillar valley are currently 12% and 52%, respectively. However, in some parts of the
33
34 forest standing mortality is >20% and cumulative mortality is as high as 50% in the last
35
36 20 years (J. Martínez-Vilalta, unpublished data). The Scots pine population studied is
37
38 more than 150 years old and has remained largely unmanaged for the past 30 years
39
40 (Hereş et al. 2012). No major insect infestation episode associated with the forest
41
42 decline in the area has been detected (Mariano Rojo, Catalan Forest Service, pers com.).
43
44 164 A mixed Holm oak – Scots pine stand with a predominantly northern aspect was
45
46 selected for this study where defoliated and non-defoliated pines were living side by
47
48 side. A total of 10 defoliated and 10 non-defoliated Scots pine trees were sampled (see
49
50 Supplementary Table S1). In order to minimize unwanted variation, all trees had a
51
52 diameter at breast height (DBH) between 25 and 50 cm (average DBH 36.08 ± 1.53 cm;
53
54
55
56
57
58
59
60

1
2
3 169 similar between defoliation classes ($P>0.05$; data not shown)) and the distance between
4
5 170 sampled trees was always >5 m (the average minimum distance was 41.99 ± 13.74 m).
6
7 171 In this study, defoliation was visually estimated relative to a completely healthy tree in
8
9 172 the same population (cf. Galiano et al. 2011). A tree was considered as non-defoliated if
10
11 173 the percentage of green needles was $>60\%$ (average green leaves of the sampled non-
12
13 174 defoliated trees = 77%) and defoliated if the percentage of green needles was $<40\%$
14
15 175 (average green leaves of the sampled defoliated trees = 26%). The average height of
16
17 176 Scots pines in the population studied was 14.1 ± 0.5 m (Poyatos et al. 2013). All
18
19 177 measurements, in combination with a continuous monitoring of the main meteorological
20
21 178 variables and soil moisture (cf. Poyatos et al. 2013 for details), were carried out during
22
23 179 2012. Sampling from defoliated trees avoided dead or dying branches (i.e., those with
24
25 180 no green leaves), so our sampling can be considered representative only of the living
26
27 181 part of the crown.

31
32 182
33

34 *Non-structural carbohydrates sampling and analysis*
35

36
37 184 Trees were sampled in March (late winter), June (late spring), August (mid summer)
38
39 185 and October (early autumn). Four organs (leaves, branches, trunk and coarse roots) were
40
41 186 sampled from every tree to measure non-structural carbohydrates (NSC). Sun-exposed
42
43 187 branches (0.5 – 1 cm of diameter with bark removed) were excised with a pole pruner
44
45 188 around noon (12:00 pm – 3:00 pm, local time) to minimize the impact of diurnal
46
47 189 variation in NSC concentrations due to photosynthetic activity (Li et al. 2008, Gruber et
48
49 190 al. 2012). One-year-old leaves were sampled from these branches. Trunk xylem at
51
52 191 breast height and coarse roots at 5-10 cm soil depth were cored to obtain sapwood.
53
54 192 Sapwood portion was visually estimated in situ from all the extracted cores. We also
55
56 193 used these cores to measure the Basal Area Increment (BAI) corresponding to the three

1
2
3 194 most recent annual rings (see Supplementary Table S1). All samples were placed
4
5 immediately in paper bags and stored in a portable cooler containing cold accumulators.
6
7 196 One of the defoliated Scots pine trees (tree 1637; see Supplementary Table S1) died
8
9 during the study period and leaves could not be sampled in August and October;
10
11 whereas branches could be sampled in August but not in October.
12
13
14 199 At the end of every sampling day, samples were microwaved for 90 s in order to stop
15
16 enzymatic activity and oven-dried for 72 h at 65 °C. Samples were then ground to fine
17
18 powder in the laboratory. Total NSC (TNSC) was defined as including free sugars
19
20 (glucose and fructose), sucrose and starch, and were analyzed following the procedures
21
22 described by Hoch et al. (2002) with some minor variations (cf. Galiano et al. 2011).
23
24
25 204 Approximately 12-14 mg of sample powder was extracted with 1.6 ml distilled water at
26
27 100 °C for 60 min. After centrifugation, an aliquot of the extract was used for the
28
29 determination of soluble sugars (glucose, fructose and sucrose), after enzymatic
30
31 conversion of fructose and sucrose into glucose (invertase from *Saccharomyces*
32
33
34 *cerevisae*) and glucose hexokinase (GHK assay reagent, I4504 and G3293, Sigma-
35
36 Aldrich). Another aliquot was incubated with an amyloglucosidase from *Aspergillus*
37
38 *niger* at 50 °C overnight, to break down all NSC (starch included) to glucose. The
39
40 concentration of free glucose was determined photometrically in a 96-well microplate
41
42 reader (Sunrise Basic Tecan, Männedorf, Switzerland) after enzymatic (GHK assay
43
44 reagent) conversion of glucose to gluconate-6-phosphate. Starch was calculated as TNSC
45
46 minus soluble sugars. All NSC values are expressed as percent dry matter. Throughout
47
48 the manuscript NSC is used to refer generically to non-structural carbohydrates, while
49
50 TNSC is used to refer specifically to the total value of NSC (sum of starch and soluble
51
52 sugars). The relationship between soluble sugars and TNSC will be expressed as
53
54 SS:TNSC. Finally, we note that due to the current uncertainty in NSC quantification
55
56
57
58
59
60

1
2
3 219 methodologies (Quentin et al., in review), our results should be considered valid in
4
5 relative terms (as used here) but not necessarily comparable to the values obtained by
6
7 other laboratories or using different methods.
8
9
10 222
11
12 223 *Hydraulic conductivity and vulnerability to xylem embolism*
13
14
15 224 Hydraulic measurements were taken on the same Scots pine individuals as NSCs,
16
17 except for one defoliated tree that could not be sampled for hydraulics. Branches and
18
19 roots were sampled in April and May 2012, respectively, for determining xylem
20
21 vulnerability curves. We selected branches and roots containing internodal segments 0.4
22
23 – 1.1 cm in diameter and ~15 cm in length. Branches were always sampled from the
24
25 exposed part of the canopy and were 3-5 years old. Root samples were taken at a soil
26
27 depth of ~20 cm and always from the down slope side of the trunk, in order to control
28
29 for differences in water availability or soil properties. Sampled branches and roots were
30
31 always longer than 40 cm and were immediately wrapped in wet cloths and stored
32
33 inside plastic bags until they were transported to the laboratory on the same day. Once
34
35 in the laboratory, samples were stored at 4 °C until their vulnerability curves were
36
37 established within less than three weeks. Right before that, all leaves distal to the
38
39 measured branch segments were removed and their total area measured with a Li-Cor
40
41 236 3100 Area Meter (Li-Cor Inc., Lincoln, NE, USA).
42
43
44 238 Vulnerability curves relating the percentage loss of hydraulic conductivity (PLC) as a
45
46 function of xylem water potential were established using the air injection method
47
48 (Cochard et al. 1992). Hydraulic conductivity (water flow per unit pressure gradient)
49
50 was measured using the XYL'EM embolism meter (Bronkhorst, Montigny-Les-
51
52 Cormeilles, France) using deionised, degassed water (Liqui-Cel Mini-Module degassing
53
54 membrane) and a pressure head of 4.5 KPa. The bark was removed from all
55
56
57
58
59
60

1
2
3 244 measurement segments and their ends were cleanly shaved with a sharp razor blade
4
5 245 before connecting to the XYL'EM apparatus.
6
7
8
9
10
11
12
13
14
15
16
17
18
19
20
21
22
23
24
25
26
27
28
29
30
31
32
33
34
35
36
37
38
39
40
41
42
43
44
45
46
47
48
49
50
51
52
53
54
55
56
57
58
59
60

246 Branch segments were rehydrated with deionized, degassed water prior to determining
247 maximum hydraulic conductivity (K_{\max}) (Espino and Schenk 2011), leading to stable
248 and consistent K_{\max} measurements. Afterwards, all segments (four to six each time)
249 were placed inside a multi-stem pressure chamber with both ends protruding. Then, we
250 raised the pressure inside the chamber to 0.1 MPa (basal value) during 10 min, lowered
251 the pressure, waited 10 min to allow the system to equilibrate, and measured hydraulic
252 conductivity under a low pressure head (4.5 kPa). Stable conductivity readings were
253 usually achieved within 3 min. These measurements were considered to represent the
254 maximum hydraulic conductivity (K_{\max}) and were used as reference conductivity (PLC
255 = 0) for the purpose of establishing vulnerability curves. We repeated this process,
256 raising the injection pressure stepwise by 0.5 MPa (roots) or 1 MPa (branches), until the
257 actual conductivity of the segment was less than 20% of K_{\max} , or when we reached 4
258 MPa. Due to technical limitations, we could not increase the pressure in the chamber
259 over 4 MPa, but only five samples (out of 38) had not reached 80% PLC at this pressure.
260 We fitted vulnerability curves with the following function (Pammenter and Van Der
261 Willigen 1998):

$$262 \text{PLC} = \frac{100}{1+\exp(a(P-P_{50}))} \quad \text{Equation 1}$$

263 In this equation, PLC is the percentage loss of hydraulic conductivity, P the applied
264 pressure, P_{50} the pressure (i.e. $-\psi$) causing a 50% PLC, and a is related to the slope of
265 the curve. Parameters were estimated with nonlinear least squares regression. Some
266 vulnerability curves lead to inconsistent results, due to technical problems, and were
267 removed from the analyses. Final sample size was 15 roots (six from defoliated and nine

1
2 268 from non-defoliated trees) and 15 branches (seven from defoliated and eight from non-
3 defoliated trees).
4
5 270 Measurements of K_{\max} were used for calculating specific hydraulic conductivity (K_S , in
6 $m^2 \text{ MPa}^{-1} \text{ s}^{-1}$), as the ratio between maximum hydraulic conductivity and mean cross-
7 sectional area of the segment (without bark); and leaf specific conductivity (K_L , in m^2
8 $\text{MPa}^{-1} \text{ s}^{-1}$), as the quotient between maximum hydraulic conductivity and distal leaf area.
9
10 272 Finally, we calculated the ratio between distal leaf area and cross-sectional area ($A_L:A_S$)
11 273 of each branch segment.
12
13 274
14
15 275
16
17
18 276
19
20
21 277 *Monitoring water potentials and native embolism*
22
23
24
25 278 We sampled one exposed branch from each of the trees that had been sampled for
26 vulnerability curves (nine defoliated and 10 non-defoliated individuals) monthly from
27
28 May to August and in October 2012. Midday and predawn leaf water potentials were
29 usually measured *in situ* on nearby defoliated and healthy pines on the same sampling
30 dates. We selected branches at least 40 cm long and containing internodal segments of
31 4-10 cm length (0.3 – 0.9 cm in diameter). Immediately following excision, branch
32 samples were placed in plastic bags with a small piece of damp paper towel, stored in a
33 bigger bag containing cold accumulators, and transported to the laboratory within 3 h.
34
35 282 All branches were sampled before 8 a.m., solar time.
36
37 286 Once in the laboratory, we measured shoot water potential on one terminal shoot per
38 sampled branch using a Scholander-type pressure chamber (PMS Instruments, Corvallis,
39 OR, USA) (except for the initial, May sampling). To measure native embolism, we cut
40 wood segments (4-10 cm in length) underwater from each sampled branch. The bark
41 was removed from the measurement segments and their ends were cleanly shaved with
42 a sharp razor blade before connecting them to the tubing system of the XYL'EM
43
44 292
45
46
47
48
49
50
51
52
53
54
55
56
57
58
59
60

1
2
3 293 apparatus to measure native hydraulic conductivity (K_i) under a pressure head of ca. 4.5
4
5 kPa. Measurement samples were rehydrated overnight and their maximum hydraulic
6
7 conductivity (K_{max}) was measured with the XYL'EM apparatus as described above. The
8
9 percentage loss of conductivity due to embolism (PLC) was computed as:
10
11
12 297
13
14
15 298 $PLC = 100 \left(1 - \frac{K_i}{K_{max}} \right)$ Equation 2
16
17
18 299
19
20 300 *Root rot pathogens*
21
22
23 301 We focused on root and butt rot pathogens as possible contributors to the decline
24
25 process observed in the forest studied. From each tree, we extracted two cores with an
26
27 increment borer, one at stump height and the other in one of the large roots. Decay
28
29 presence was noted and cores were kept in sterile conditions. Within 48 hours, they
30
31 were placed onto Hagem medium amended with benomyl (10 mg/l) and cloramphenicol
32
33 (200 mg/l). Plates were checked weekly during the following 3 months, and any
34
35 mycelia growth was sub-cultured. Identification of fungal isolates was first attempted
36
37 by sequencing the ITS region. Some of our isolates showed an equally low similarity
38
39 (95%) to other isolates classified as either *Onnia tomentosa* (Fr.) P. Karst. or *O.*
40
41 *circinata* (Fr.) P. Karst. in reference databases such as Genbank or UNITE. We
42
43 identified our cultures as *Onnia* spp., as morphological characters in culture and
44
45 comparison with reference cultures from CBS-KNAW Fungal Biodiversity Centre
46
47 (CBS 246.30 *Onnia circinata*, CBS 278.55 *Onnia tomentosa*) did not yield a conclusive
48
49 identification.
50
51
52 315 We found signs of fungi infection after the cultivation of the extracted cores in seven
53
54 pines; three of them were non-defoliated and the other four were defoliated (see
55
56
57 316 Supplementary Table S1). One defoliated and one non-defoliated tree were infected by
58
59
60 317

1
2
3 318 a heart rot fungi (*Porodaedalea pini* (Brot.) Murrill). These fungi mainly cause
4
5 heartwood decay with no major known physiological effects (Garbelotto 2004), so we
6
7 considered these two trees as 'non-infected' in our analyses. The other trees (two non-
8
9 defoliated and three defoliated) were infected by *Onnia* sp., which causes root rot and
10
11 physiological impairment, and we considered those trees as 'infected' in subsequent
12
13 analyses.
14
15
16 324
17
18 325 *Data analysis*
19
20
21 326 We used different types of linear models to test the effects of defoliation and fungal
22
23 infection on the measured response variables (RV). In each case we included the main
24
25 covariates (measured organ and sampling month, as appropriate) and the most
26
27 biologically plausible interactions. Please note that model complexity, in terms of the
28
29 number of interactions that could be included, is subject to sample size limitations.
30
31 331 Preliminary analyses showed that DBH effects were never significant in the models and
32
33 therefore were not included in the final models reported here. General linear models
34
35 were fitted to study the effects of defoliation class (two levels: defoliated or non-
36
37 defoliated) and infection occurrence (two levels: infected or non-infected) on K_L , $A_L:A_S$,
38
39 BAI and root and trunk sapwood depths. Separate linear models were fitted for each of
40
41 the five response variables (see Supplementary data, equation 1). Linear mixed models
42
43 were used to analyze vulnerability curve parameters (a and P_{50}) and K_S as a function of
44
45 defoliation class, organ (branch or root) and infection occurrence. Tree identity was
46
47 included in the models as a random factor (see Supplementary data, equation 2). Similar
48
49 mixed models were used to analyze shoot water potential, PLC, TNSC and SS:TNSC as
50
51 a function of defoliation class, sampling date, organ (only for TNSC and SS:TNSC),
52
53 and infection occurrence, including again tree identity as a random factor (see
54
55
56
57
58
59
60

1
2
3 343 Supplementary data, equation 3 and equation 4). Finally, starch concentration in roots
4
5 344 was also analysed using similar models (without the organ effect) to study in detail the
6
7 345 impact of root rot pathogens on this NSC fraction and how it developed over time (and
8
9 346 hence in this model we included the interaction between defoliation class, infection
10
11 347 occurrence and sampling date) (see Supplementary data, equation 5).

12
13
14 348 Variables K_S , K_L , $A_L:A_S$, TNSC and root and trunk sapwood depth were log-transformed,
15
16 349 and starch concentration in roots was square root-transformed, to achieve normality
17
18 350 prior to all analyses. All analyses were carried out with R Statistical Software version
19
20 351 3.1.0 (R Core Team 2014) using the lm and lme functions.

21
22
23 352 **Results**

24
25
26 353 *Meteorological conditions*

27
28
29 354 The summer of 2012 was particularly dry and warm compared to the climatic average
30
31 355 for the period 1951-2010: average air temperature (June-August) was 20.56 °C and total
32
33 356 precipitation only 56 mm (Fig. 1), compared to climatic values (1951-2010) of 19.30 °C
34
35 357 and 135.23 mm, respectively. High values of daytime-averaged temperatures and VPD's
36
37 358 (vapour pressure deficit) occurred in mid-August, followed by very low SWC (soil
38
39 359 water content) values ($\sim 0.08 \text{ m}^3 \text{ m}^{-3}$) at the beginning of September, compared to a
40
41 360 spring maximum soil moisture of $0.33 \text{ m}^3 \text{ m}^{-3}$ (Fig. 1).

42
43 361

44
45
46 362 *Non-structural carbohydrates*

47
48
49 363 Concentrations of total non-structural carbohydrates varied among tree organs, in the
50
51 364 following order: TNSC (leaves) > TNSC (branches) > TNSC (roots) > TNSC (trunk) (Fig.
52
53 365 2; Table 1). In general, non-defoliated Scots pine trees showed higher concentrations of
54
55 366 TNSC throughout the study period and across all organs (Fig. 2). TNSC values

1
2
3 367 increased from March to June (except for leaves of defoliated pines) to reach a seasonal
4
5 368 peak and then declined in August. Seasonal variation in TNSC was greater in leaves,
6
7 369 especially for non-defoliated pines, which showed a more than fourfold decline in
8
9 370 TNSC between the June peak and the minimum value in August. Post-drought October
10
11 371 TNSC only slightly increased in trunks and leaves (Fig. 2). Infection by fungal
12
13 372 pathogens was not associated with significant differences in TNSC levels in any organ
14
15 373 or month (Table 1).

16
17
18 374 The ratio of soluble sugars to TNSC (SS:TNSC) differed among tree organs but showed
19
20 375 consistent seasonal dynamics across organs (Fig. 2, Table 1). The value of SS:TNSC
21
22 376 declined slightly from March to June, it increased in August, especially in leaves, and
23
24 377 then declined in October. In August, SS:TNSC values were above 0.8 for all organs and
25
26 378 defoliation classes, indicating that most of the TNSC were in the form of soluble sugars
27
28 379 (Fig. 2). Starch levels at peak drought were virtually depleted in leaves (i.e. SS:TNSC
29
30 380 was nearly 1). Moreover, there were significant differences in SS:TNSC between
31
32 381 defoliation classes in some organs and months, whereby defoliated pines tended to show
33
34 382 higher SS:TNSC values before the onset of drought but similar or lower values in
35
36 383 August (Fig. 2, Table 1). No differences in SS:TNSC were observed associated to fungi
37
38 384 infection (Table 1).

39
40
41 385 Throughout the season, root starch tended to be lower in defoliated pines compared to
42
43 386 non-defoliated ones (Fig. 3). Root rot infection was associated with higher root starch
44
45 387 levels in non-defoliated pines, but this effect was not observed in defoliated pines (Fig.
46
47 388 3, Table 1). The triple interaction between month, defoliation and infection was
48
49 389 statistically significant (Table 1). Interestingly, our results show that root starch
50
51 390 concentration in October was virtually depleted in infected, defoliated pines, and it was
52
53 391 much lower than in non-infected ones (Fig. 3).

1
2
3
4
5
6
7
8
9
10
11
12
13
14
15
16
17
18
19
20
21
22
23
24
25
26
27
28
29
30
31
32
33
34
35
36
37
38
39
40
41
42
43
44
45
46
47
48
49
50
51
52
53
54
55
56
57
58
59
60

392
393 *Vulnerability curves and hydraulic properties*

394 Roots were more vulnerable to embolism than branches, reaching 50% PLC slightly
395 below -2 MPa, compared to a value close to -3 MPa for branches (Fig. 4). This effect
396 was statistically significant (overall *P*-value for Organ = 0.0062 in a least significant
397 means multiple comparison), although the difference was not significant for all the
398 combinations of defoliation and infections classes (cf. Table 2). The vulnerability to
399 embolism of branches was similar between defoliation classes (Fig. 4b, Table 2). In
400 roots, there was no difference between defoliation classes in P_{50} , but the slope of the
401 vulnerability curve was steeper in defoliated trees (Table 2). This result implies that the
402 roots of non-defoliated pines would begin to lose conductivity at higher (i.e., closer to
403 zero) water potentials than those of defoliated individuals, but the latter would lose
404 conductivity faster than non-defoliated pines as water potentials declines (Fig. 4a).
405 Infection did not affect vulnerability to xylem embolism (Table 2).

406 No differences in specific hydraulic conductivity (K_s) were found between roots and
407 branches (Table 2), possibly due, at least in part, to the large variability in K_s observed
408 for roots. Likewise, there were no significant differences in either K_s , K_L , or $A_L:A_s$
409 between defoliated and non-defoliated pines (Table 2). However, we found lower
410 branch K_L in infected trees (Table 2).

411

412 *Water potentials and native embolism*

413 Shoot water potentials measured in the morning, at the time of sampling for PLC
414 measurements, increased from June to July (Fig. 5b, Table 3), consistent with the
415 rainfall events occurring in late June (Fig. 1). Afterwards, water potentials declined
416 sharply down to values around -2 MPa in August, coinciding with the driest part of the

1
2
3 417 study period. These water potentials were usually between the corresponding predawn
4
5 and midday shoot water potentials measured in simultaneous sampling campaigns in
6
7 nearby Scots pine individuals (Fig. 5c). We did not find any significant effect of
8
9 defoliation or infection on water potential (Table 3).
10

11
12 421 Native PLC varied significantly among sampling dates, following the variation in shoot
13
14 water potentials. PLC was particularly low in July, with values around 20%, and it was
15
16 highest in August, with average values around 65% (Fig. 5a, Table 3). In August, six
17
18 branches (four from non-defoliated, and two from defoliated pines) showed PLC values
19
20 above 85%. Native embolism was not significantly different between defoliation or
21
22 infection classes (Table 3), except for October when non-defoliated pines showed
23
24 higher PLC (Fig. 5b) ($P = 0.048$).
25
26

27
28 428
29
30

31
32 429 *Basal area increment and sapwood depth*
33
34

35
36 430 We found a marginally significant reduction of BAI associated with defoliation ($P =$
37
38 0.064) and this effect tended to be larger in infected trees as shown by the marginally
39
40 significant ($P = 0.083$) interaction between defoliation and infection (Fig. 6a).
41
42

43
44 433 Trunk sapwood depth showed patterns similar to those for BAI, but with significantly
45
46 lower values for defoliated and infected individuals (Fig. 6b). Finally, infected trees
47
48 showed a significantly lower root sapwood depth compared to non-infected trees ($P =$
49
50 0.039), regardless of defoliation class; whereas defoliation had no significant effect on
51
52 root sapwood depth (Fig. 6c) ($P = 0.89$).
53
54

55
56 438
57
58

59
60 439 **Discussion**

61
62 440 Our results show that both high levels of embolism and low carbohydrate reserves
63
64 occurred in the studied trees during a particularly dry summer. In addition, we show that
65
66

1
2 442 defoliation was more associated with reduced carbohydrate reserves than with greater
3 443 hydraulic impairment at the branch level. We also report that drought-induced
4 444 defoliation and infection by a root rot fungus occur independently, but they both interact
5 445 to determine the mode of physiological failure in Scots pine at the dry edge of its
6 446 distribution. We note, however, that some of these results (particularly those regarding
7 447 pathogen infection) should be interpreted with caution due to the low sample size.
8
9
10
11
12
13
14
15
16
17
18
19
20
21
22
23
24
25
26
27
28
29
30
31
32
33
34
35
36
37
38
39
40
41
42
43
44
45
46
47
48
49
50
51
52
53
54
55
56
57
58
59
60

448
449 *Defoliation is associated with lower carbon availability, but not with higher hydraulic
450 impairment at the branch level*

451 We found no consistent differences between defoliated and non-defoliated pines in
452 terms of their vulnerability to embolism according to P_{50} values. This is consistent with
453 previous studies comparing Scots pine populations suffering different levels of drought-
454 induced decline in the same area (Martínez-Vilalta et al. 2002). Although we found
455 steeper vulnerability curves for roots of defoliated pines, which would yield
456 comparatively higher root PLC at water potentials lower than *ca.* -2 MPa (Fig. 4a),
457 these conditions only occur during exceptional droughts (Poyatos et al. 2013). In
458 addition, branch-level leaf K_S and $A_L:A_S$ were similar for defoliated and non-defoliated
459 pines, in contrast with different values observed across Scots pine populations within
460 the same study area (Martínez-Vilalta and Piñol 2002) and with the lower $A_L:A_S$
461 reported at the tree level for defoliated pines (Poyatos et al. 2013). It should be
462 emphasized, however, that our sampling design is representative at the branch level, but
463 not necessarily at the whole crown level, as we were forced to sample living (as
464 opposed to random) branches in heavily defoliated crowns.

465 It is also interesting to note that our results show a slightly higher branch vulnerability
466 to embolism compared to the P_{50} of ~3.2 MPa reported previously for the same

1
2 population (Martínez-Vilalta and Piñol 2002). This result may be related to some sort of
3 filtering at the population level (i.e., preferential mortality of pines with higher
4 resistance to embolism) or a by-product of the large variability in P_{50} observed across
5 branches. But it is also possible that vulnerability to embolism may be increasing over
6 time as a result of repeated droughts (i.e. cavitation fatigue; Hacke et al. (2001)), as it
7 has been reported in the case of aspen die-off (Anderegg et al. 2013b).
8
9

10 The decline in PLC observed after a rainy period in July (Fig. 5a) suggests some partial
11 embolism reversal (e.g. McCulloh et al. 2011), but we cannot rule out the possibility
12 that sampling artefacts may be causing an overestimation of this PLC recovery (e.g.
13 Sperry 2013). Although our results imply that defoliation may be relatively effective in
14 avoiding further increases in branch PLC, maximum PLC values were still within a
15 range (*ca.* 50-90%) associated with canopy dieback in several angiosperms (Hoffmann
16 et al. 2011, Anderegg et al. 2012, Anderegg et al. 2013b, Nardini et al. 2013) and
17 gymnosperms (Klein et al. 2012, Plaut et al. 2012). Overall, these results also suggest
18 that the steeper declines in whole-plant hydraulic conductance observed for defoliated
19 pines during drought (Poyatos et al. 2013) may occur primarily belowground, as
20 observed in other pine species prior to death (Plaut et al. 2013).
21
22

23
24 484
25 Defoliated pines showed consistently lower TNSC values than non-defoliated pines for
26 most combinations of organ and season, as already observed in early autumn
27 measurements of stem TNSC in other declining Scots pine populations (Galiano et al.
28 2011), including the study site (Poyatos et al. 2013). Interestingly, we did not observe
29 increased TNSC in leaves of defoliated pines, despite their higher assimilation rates
30 (Mencuccini et al., unpublished data). TNSC decreased in all organs during drought,
31
32
33
34
35
36
37
38
39
40
41
42
43
44
45
46
47
48
49
50
51
52
53
54
55
56
57
58
59
60

1
2
3 491 and most dramatically in leaves, tracking the seasonality of gas exchange (Poyatos et al.
4
5 492 2013).

6
7
8 493 The observed seasonal variation of the fraction of soluble sugars (SS:TNSC) (Fig. 2) is
9
10 494 consistent with starch concentration building up prior to bud-break and then decreasing
11
12 495 during the summer period (Hoch and Körner 2003, Gruber et al. 2012). During August,
13
14 496 the greater mobilization of starch to soluble sugars could be attributed to several causes,
15
16 497 including osmoregulation (Sala et al. 2012), the de novo synthesis of carbon-rich
17
18 498 compounds into defence against root rot pathogens (Oliva et al. 2012), the energy-
19
20 499 dependent process of embolism repair (Brodersen and McElrone 2013) and the growth
21
22 500 of new tissue. The two latter processes are consistent with the reduction of native
23
24 501 embolism after August, reaching pre-drought values in October (Fig. 5a).

25
26
27 502 Despite the combination of drought and defoliation, our results did not show a complete
28
29 503 depletion of TNSC in any of the organs studied (Fig. 2), even in the tree that died during
30
31 504 the monitoring period (data not shown). Values of trunk TNSC as low as 0.1% were
32
33 505 measured in Scots pine one year prior to death in a nearby population (Galiano et al.
34
35 506 2011) while our trunk TNSC values were always >0.4%. Experimental studies on
36
37 507 conifer saplings (Hartmann et al. 2013b), including pine species (Mitchell et al. 2013),
38
39 508 have found evidence for drastic reductions in TNSC (especially starch) in stems and/or
40
41 509 roots at mortality, without actually showing completely depleted carbohydrate storage.
42
43 510 Phloem impairment may preclude the translocation of NSC and its availability for the
44
45 511 maintenance of xylem transport or for the production of defence compounds (Sala et al.
46
47 512 2010, Sevanto et al. 2013, Hartmann et al. 2013a). A recent modelling analysis in the
48
49 513 same study system predicts slow, but not disrupted, phloem transport under extreme
50
51 514 drought (Mencuccini et al., unpublished data).

52
53
54 515

1
2 516 *Root rot pathogens exacerbate hydraulic and carbon-related constraints at the tree*
3
4 517 *level*

5
6 518 We did not find a clear BAI reduction in *Onnia*-infected trees (Fig. 6a), contrary to
7
8 519 other studies reporting growth reductions caused by root rot pathogens from the
9
10 520 *Armillaria* (Cruickshank et al. 2011) and *Heterobasidion* genus (Oliva et al. 2012).

11
12 521 Although the interaction between infection and defoliation was only marginally
13
14 522 significant, the trend towards lower BAI in trees that were both defoliated and infected
15
16 523 would be consistent with the reduced sapwood depth observed in these trees (Fig. 6b).

17
18 524 Hence, post-drought recovery of xylem specific hydraulic conductivity would be
19
20 525 severely constrained in the long-term. Lower sapwood depth in the roots of infected
21
22 526 trees (Fig. 6c), could be the ultimate consequence of the decay progress, due to the
23
24 527 reduction of tree growth caused by the formation of a reaction zone (Oliva et al. 2012).

25
26 528 Infection-driven reductions in sapwood depth in roots (and in the trunk of infected,
27
28 529 defoliated trees) may also result in lower tissue capacitance and a decreased ability to
29
30 530 buffer short-term variations in water potential under drought (McCulloh et al. 2014).

31
32 531 Even though *Onnia* infection did not affect the vulnerability to embolism, it was
33
34 532 associated with reduced K_L , particularly in defoliated pines (Table 2). Hence, infection
35
36 533 by a root rot pathogen likely exacerbated hydraulic constraints through effects on
37
38 534 growth and sapwood depth but also more directly through its impact on hydraulic
39
40 535 conductivity.

41
42 536 Our results show a complex picture of the root rot infection effects on NSC pools. We
43
44 537 did not find any evidence for consistent reductions in TNSC across tree organs
45
46 538 associated with *Onnia* infection. However, for non-defoliated pines, infection appeared
47
48 539 to drive starch accumulation in roots, rather than depletion, possibly as a response to
49
50 540 increased sink strength in the roots associated to higher C demand (de novo synthesis of

1
2 541 defence compounds; Oliva et al. 2014). Presumably, defoliated pines were so severely
3 542 carbon-limited that this starch sink in the roots could not be maintained, and they ended
4 543 the year with extremely low levels of starch in roots (Fig. 3). These findings are in line
5 544 with a recently proposed framework, which postulates that the net effect of the infection
6 545 by a necrotrophic pathogen, such as *Onnia*, is strongly dependent on tree C availability
7 546 and the timing of drought events (Oliva et al. 2014).
8
9
10
11
12
13
14
15
16
17
18
19
20
21
22
23
24
25
26
27
28
29
30
31
32
33
34
35
36
37
38
39
40
41
42
43
44
45
46
47
48
49
50
51
52
53
54
55
56
57
58
59
60

547
548 *A complex pathway to mortality*

549 In this final section we synthesize our current understanding on the process of drought-
550 induced mortality in the study area, from the perspective of the comparison of
551 coexisting defoliated and healthy individuals, using the information gathered here and
552 in other studies conducted at the same site (Fig. 7). Drought-induced defoliation is
553 associated with drier microenvironments (Vilà-Cabrera et al. 2013) and with steeper
554 reductions of whole-plant hydraulic conductance during seasonal drought (Poyatos et al.
555 2013). Hydraulic constraints may be related to higher vulnerability to embolism in roots
556 (steeper vulnerability curves) and can be magnified by cavitation fatigue following
557 repeated droughts. Defoliation and prolonged periods of near complete stomatal closure
558 both contribute to reduce NSC in defoliated trees (Poyatos et al. 2013). Defoliated trees
559 appear to enter a death spiral in which reduced C assimilation constrains radial growth
560 (Hereş et al. 2012) and crown development (Poyatos et al. 2013). Root rot fungi may
561 further damage hydraulic function through direct effects on sapwood depth and
562 cumulative growth reductions. Moreover, the demand for C-rich compounds for
563 osmoregulation, hydraulic repair and defence against root rot infection may contribute
564 to the depletion of C reserves in defoliated pines, possibly increasing the minimum C
565 threshold for tree survival and hence accelerating tree mortality (Oliva et al. 2014). It

1
2
3 566 remains to be established whether the framework outlined in Fig. 7, which has been
4 developed for only one species in a given region, can be applied to other species and
5 study systems. Overall, our study reflects the intertwined nature of physiological
6 mechanisms leading to drought-induced mortality (McDowell et al. 2011) and the
7 inherent difficulty of isolating their contribution under field conditions.
8
9
10
11
12
13
14
15

16 571
17

18 572 **Supplementary data** 19

20 573 Supplementary data for this article are available at Tree Physiology Online.
21
22
23
24

25 575 **Acknowledgements** 26

27 576 We would like to thank L. Galiano and T. Rosas for assistance in field sampling and
28 carbohydrates analysis. We also thank all the staff from the Poblet Forest Natural
29 Reserve for allowing us to carry out research at the “Barranc del Tillar” and for their
30 logistic support in the field. The comments by Rick Meinzer and two anonymous
31
32
33
34
35
36
37
38
39
39
40
41
42
43
44
45
46
47
48
49
50
51
52
53
54
55
56
57
58
59
59
60

580
581
582
583
584
585
586
587
588
589
590

582 **Conflict of interest**

583 None declared.

585 **Funding**

586 Competitive grants CGL2010-16373 and CSD2008-0004, a Juan de la Cierva
587 postdoctoral fellowship awarded to R.P., and a FPU doctoral fellowship through the
588 Spanish Ministry of Education, Culture and Sport awarded to D.A.

591 **References**

592 Adams HD, Germino MJ, Breshears DD, Barron-Gafford GA, Guardiola-Claramonte M,
593 Zou CB, Huxman TE (2013) Nonstructural leaf carbohydrate dynamics of *Pinus*
594 *edulis* during drought-induced tree mortality reveal role for carbon metabolism
595 in mortality mechanism. *New Phytol* 197:1142-1151.

596 Allen CD, Macalady AK, Chenchouni H, Bachelet D, McDowell N, Vennetier M,
597 Kitzberger T, Rigling A, Breshears DD, Hogg EH (2010) A global overview of
598 drought and heat-induced tree mortality reveals emerging climate change risks
599 for forests. *For Ecol Manag* 259:660-684.

600 Anderegg WRL, Berry JA, Smith DD, Sperry JS, Anderegg LDL, Field CB (2012) The
601 roles of hydraulic and carbon stress in a widespread climate-induced forest die-
602 off. *Proc. Nat. Acad. Sci* 109:233-237.

603 Anderegg WRL, Kane JM, Anderegg LDL (2013a) Consequences of widespread tree
604 mortality triggered by drought and temperature stress. *Nature Clim Change*
605 3:30-36.

606 Anderegg WRL, Plavcová L, Anderegg LDL, Hacke UG, Berry JA, Field CB (2013b)
607 Drought's legacy: multiyear hydraulic deterioration underlies widespread aspen
608 forest die-off and portends increased future risk. *Glob Change Biol* 19:1188-
609 1196.

610 Bonan, GB (2008) Forests and climate change: forcings, feedbacks, and the climate
611 benefits of forests. *Science* 320:1444-1449.

612 Brodersen CR, McElrone, AJ (2013) Maintenance of xylem network transport capacity:
613 a review of embolism repair in vascular plants. *Front Plant Sci* 4.

614 Brodribb TJ, Cochard H (2009) Hydraulic failure defines the recovery and point of
615 death in water-stressed conifers. *Plant Physiol* 149:575-584.

1
2
3 616 Carnicer J, Coll M, Ninyerola M, Pons X, Sánchez G, Peñuelas J (2011) Widespread
4
5 617 crown condition decline, food web disruption, and amplified tree mortality with
6
7 618 increased climate change-type drought. *Proc. Nat. Acad. Sci* 108:1474-1478.
8
9 619 Choat B, Jansen S, Brodribb TJ, Cochard H, Delzon S, Bhaskar R, Bucci SJ, Feild TS,
10
11 620 Gleason SM, Hacke UG, Jacobsen AL, Lens F, Maherli H, Martínez-Vilalta J,
12
13 621 Mayr S, Mencuccini M, Mitchell PJ, Nardini A, Pittermann J, Pratt RB, Sperry
14
15 622 JS, Westoby M, Wright IJ, Zanne AE (2012) Global convergence in the
16
17 623 vulnerability of forests to drought. *Nature* 491:752-755.
18
19
20 624 Cochard H, Cruiziat P, Tyree MT (1992) Use of Positive Pressures to Establish
21
22 625 Vulnerability Curves. Further Support for the Air-Seeding Hypothesis and
23
24 626 Implications for Pressure-Volume Analysis. *Plant Physiol* 100:205-209.
25
26
27 627 Cruickshank MG, Morrison DJ, Lalumière A (2011) Site, plot, and individual tree yield
28
29 628 reduction of interior Douglas-fir associated with non-lethal infection by
30
31 629 Armillaria root disease in southern British Columbia. *For Ecol Manag* 261:297-
32
33 630 307.
34
35
36 631 Desprez-Loustau ML, Marçais B, Nageleisen LM, Piou D, Vannini A (2006) Interactive
37
38 632 effects of drought and pathogens in forest trees. *Ann Sci For* 63:597-612.
39
40
41 633 Espino S, Schenk HJ (2011) Mind the bubbles: achieving stable measurements of
42
43 634 maximum hydraulic conductivity through woody plant samples. *J Exp Bot*
44
45 635 62:1119-1132.
46
47
48 636 Galiano L, Martínez-Vilalta J, Lloret F (2011) Carbon reserves and canopy defoliation
49
50 637 determine the recovery of Scots pine 4 yr after a drought episode. *New Phytol*
51
52 638 190:750-759.
53
54
55 639 Garbelotto M (2004) Root and butt rot diseases. In: Burley J, Evan J, Youngquist JA
56
57 640 (eds) *The encyclopedia of forest sciences*. Elsevier, Oxford, pp 750-758.
58
59
60

1
2
3 641 Gaylord ML, Kolb TE, Pockman WT, Plaut JA, Yepez EA, Macalady AK, Pangle RE,
4
5 642 McDowell NG (2013) Drought predisposes piñon-juniper woodlands to insect
6
7 643 attacks and mortality. *New Phytol* 198:567-578.
8
9 644 Gruber A, Pirkebner D, Florian C, Oberhuber W (2012) No evidence for depletion of
10
11 645 carbohydrate pools in Scots pine (*Pinus sylvestris* L.) under drought stress. *Plant*
12
13 646 *Biol* 14:142-148.
14
15
16 647 Hacke UG, Stiller V, Sperry JS, Pittermann J, McCulloh KA (2001) Cavitation fatigue.
17
18 648 Embolism and refilling cycles can weaken the cavitation resistance of xylem.
19
20 649 *Plant Physiol* 125:779-786.
21
22
23 650 Hartmann H, Ziegler W, Kolle O, Trumbore S (2013a) Thirst beats hunger-declining
24
25 651 hydration during drought prevents carbon starvation in Norway spruce saplings.
26
27 652 *New Phytol* 200:340-349.
28
29
30 653 Hartmann H, Ziegler W, Trumbore S (2013b) Lethal drought leads to reduction in
31
32 654 nonstructural carbohydrates in Norway spruce tree roots but not in the canopy.
33
34 655 *Funct Ecol* 27:413-427.
35
36
37 656 Heres A-M, Martínez-Vilalta J, López BC (2012) Growth patterns in relation to
38
39 657 drought-induced mortality at two Scots pine (*Pinus sylvestris* L.) sites in NE
40
41 658 Iberian Peninsula. *Trees-Struct Funct* 26:621-630.
42
43
44 659 Heres A-M, Voltas J, López BC, Martínez-Vilalta J (2013) Drought-induced mortality
45
46 660 selectively affects Scots pine trees that show limited intrinsic water-use
47
48 661 efficiency responsiveness to raising atmospheric CO₂. *Funct Plant Biol* 41:244-
49
50 662 256.
51
52
53 663 Hereter A, Sánchez JR (1999) Experimental areas of Prades and Montseny. In: Rodà F,
54
55 664 Retana J, Gracia CA, Bellot J (eds) *Ecology of Mediterranean evergreen oak*
56
57 665 forests. Springer, Berlin, Heidelberg, pp 15-27.
58
59
60

1
2
3 666 Hoch G, Körner C (2003) The carbon charging of pines at the climatic treeline: a global
4
5 667 comparison. *Oecologia* 135:10-21.
6
7 668 Hoch G, Popp M, Körner C (2002) Altitudinal increase of mobile carbon pools in *Pinus*
8
9 669 *cembra* suggests sink limitation of growth at the Swiss treeline. *Oikos* 98:361-
10
11 670 374.
12
13
14 671 Hoffmann WA, Marchin RM, Abit P, Lau OL (2011) Hydraulic failure and tree dieback
15
16 672 are associated with high wood density in a temperate forest under extreme
17
18 673 drought. *Glob Change Biol* 17:2731-2742.
19
20
21 674 Hubbard RM, Rhoades CC, Elder K, Negron J (2013) Changes in transpiration and
22
23 675 foliage growth in lodgepole pine trees following mountain pine beetle attack and
24
25 676 mechanical girdling. *For Ecol Manag* 289:312-317.
26
27
28 677 IPCC. 2013 Climate Change 2013: The Physical Science Basis. Contribution of
29
30 678 Working Group I to the Fifth Assessment Report of the Intergovernmental Panel
31
32 679 on Climate Change (IPCC). Cambridge University Press, Cambridge, UK and
33
34 680 New York, NY, USA, 1535 pp.
35
36
37 681 Klein T, Di Matteo G, Rotenberg E, Cohen S, Yakir D (2012) Differential
38
39 682 ecophysiological response of a major Mediterranean pine species across a
40
41 683 climatic gradient. *Tree Physiol* 33(1):26-36.
42
43
44 684 La Porta N, Capretti P, Thomsen IM, Kasanen R, Hietala AM, Von Weissenberg K
45
46 685 (2008) Forest pathogens with higher damage potential due to climate change in
47
48 686 Europe. *Can J Plant Pathol* 30:177-195.
49
50
51 687 Li MH, Xiao WF, Wang SG, Cheng GW, Cherubini P, Cai XH, Liu XL, Wang XD,
52
53 688 Zhu WZ (2008) Mobile carbohydrates in Himalayan treeline trees I. Evidence
54
55 689 for carbon gain limitation but not for growth limitation. *Tree Physiol* 28:1287-
56
57 690 1296.
58
59
60

1
2
3 691 Martínez-Vilalta J, Lloret F, Breshears DD (2012) Drought-induced forest decline:
4
5 692 causes, scope and implications. *Biol Letters* 8:689-691.
6
7 693 Martínez-Vilalta J, Piñol J (2002) Drought-induced mortality and hydraulic architecture
8
9 694 in pine populations of the NE Iberian Peninsula. *For Ecol Manag* 161:247-256.
10
11 695 Matthias D, Beat W, Christof B, Matthias B, Mathias C, Beat F, Urs G, Andreas R
12
13 696 (2007) Linking increasing drought stress to Scots pine mortality and bark beetle
14
15 697 infestations. *Scientific World Journal* 7:231-239.
16
17
18 698 McCulloh KA, Johnson DM, Meinzer FC, Lachenbruch B (2011) An annual pattern of
19
20 699 native embolism in upper branches of four tall conifer species. *Am J Bot*
21
22 700 98:1007-1015.
23
24
25 701 McCulloh KA, Johnson DM, Meinzer FC, Woodruff DR (2014) The dynamic pipeline:
26
27 702 hydraulic capacitance and xylem hydraulic safety in four tall conifer species.
28
29 703 *Plant Cell Environ* 37:1171-1183.
30
31
32 704 McDowell N, Pockman WT, Allen CD, Breshears DD, Cobb N, Kolb T, Plaut J, Sperry
33
34 705 J, West A, Williams DG, Yepez EA (2008) Mechanisms of plant survival and
35
36 706 mortality during drought: why do some plants survive while others succumb to
37
38 707 drought? *New Phytol* 178:719-739.
39
40
41 708 McDowell NG (2011) Mechanisms linking drought, hydraulics, carbon metabolism, and
42
43 709 vegetation mortality. *Plant Physiol* 155:1051-1059.
44
45
46 710 McDowell NG, Beerling DJ, Breshears DD, Fisher RA, Raffa KF, Stitt M (2011) The
47
48 711 interdependence of mechanisms underlying climate-driven vegetation mortality.
49
50 712 *Trends Ecol Evol* 26:523-532.
51
52 713 McDowell NG, Sevanto S (2010) The mechanisms of carbon starvation: how, when, or
53
54 714 does it even occur at all? *New Phytol* 186:264-266.
55
56
57
58
59
60

1
2
3 715 Mitchell PJ, O'Grady AP, Tissue DT, White DA, Ottenschlaeger ML, Pinkard EA (2013)
4
5 716 Drought response strategies define the relative contributions of hydraulic
6
7 717 dysfunction and carbohydrate depletion during tree mortality. *New Phytol*
8
9 718 197:862-872.
10
11
12 719 Nardini A, Battistuzzo M, Savi T (2013) Shoot desiccation and hydraulic failure in
13
14 temperate woody angiosperms during an extreme summer drought. *New Phytol*
15
16 721 200:322-329.
17
18
19 722 Oliva J, Camarero J, Stenlid J (2012) Understanding the role of sapwood loss and
20
21 reaction zone formation on radial growth of Norway spruce (*Picea abies*) trees
22
23 decayed by *Heterobasidion annosum* s.l. *For Ecol Manag* 274:201-209.
24
25
26 725 Oliva J, Stenlid J, Martínez-Vilalta J (2014) The effect of fungal pathogens on the water
27
28 and carbon economy of trees: implications for drought-induced mortality. *New*
29
30 727 *Phytol* DOI: 10.1111/nph.12857.
31
32
33 728 Pammeter NW, Van Der Willigen C (1998) A mathematical and statistical analysis of
34
35 the curves illustrating vulnerability of xylem to cavitation. *Tree Physiol* 18:589-
36
37 593.
38
39 731 Piper FI (2011) Drought induces opposite changes in the concentration of non-structural
40
41 carbohydrates of two evergreen *Nothofagus* species of differential drought
42
43 733 resistance. *Ann Sci For* 68:415-424.
44
45
46 734 Plaut JA, Wadsworth WD, Pangle R, Yepez EA, McDowell NG, Pockman WT (2013)
47
48 735 Reduced transpiration response to precipitation pulses precedes mortality in a
49
50 piñon-juniper woodland subject to prolonged drought. *New Phytol* 200:375-387.
51
52
53 737 Plaut JA, Yepez EA, Hill J, Pangle R, Sperry JS, Pockman WT, McDowell NG (2012)
54
55 738 Hydraulic limits preceding mortality in a piñon-juniper woodland under
56
57 739 experimental drought. *Plant Cell Environ* 35:1601-1617.
58
59
60

1
2
3 740 Poyatos R, Aguadé D, Galiano L, Mencuccini M, Martínez-Vilalta J (2013) Drought-
4
5 induced defoliation and long periods of near-zero gas exchange play a key role
6
7 742 in accentuating metabolic decline of Scots pine. *New Phytol* 200:388-401.
8
9 743 R Core Team (2014). R: A language and environment for statistical computing. R
10
11 744 Foundation for Statistical Computing, Vienna, Austria. URL [http://R-
12
13
14
15
16
17
18
19
20
21
22
23
24
25
26
27
28
29
30
31
32
33
34
35
36
37
38
39
40
41
42
43
44
45
46
47
48
49
50
51
52
53
54
55
56
57
58
59
60
745 project.org/.](http://R-project.org/)

746 Sala A, Piper F, Hoch G (2010) Physiological mechanisms of drought induced tree
747 mortality are far from being resolved. *New Phytol* 186:274-281.

748 Sala A, Woodruff DR, Meinzer FC (2012) Carbon dynamics in trees: feast or famine?
749 *Tree Physiol* 32:764-775.

750 Sevanto S, McDowell NG, Dickman LT, Pangle R, Pockman WT (2013) How do trees
751 die? A test of the hydraulic failure and carbon starvation hypotheses. *Plant Cell
752 Environ* 37:153-161.

753 Sperry J (2013) Cutting-edge research or cutting-edge artefact? An overdue control
754 experiment complicates the xylem refilling story. *Plant Cell Environ* 36:1916-
755 1918.

756 Urli M, Porté AJ, Cochard H, Guengant Y, Burlett R, Delzon S (2013) Xylem embolism
757 threshold for catastrophic hydraulic failure in angiosperm trees. *Tree Physiol*
758 33:672-683.

759 Van Mantgem PJ, Stephenson NL, Byrne JC, Daniels LD, Franklin JF, Fule PZ,
760 Harmon ME, Larson AJ, Smith JM, Taylor AH (2009) Widespread increase of
761 tree mortality rates in the western United States. *Science* 323:521-524.

762 Vilà-Cabrera A, Martínez-Vilalta J, Galiano L, Retana J (2013) Patterns of forest
763 decline and regeneration across Scots pine populations. *Ecosystems* 16:323-335.

1
2
3 764 Williams AP, Allen CD, Macalady AK, Griffin D, Woodhouse CA, Meko DM,
4
5 765 Swetnam TW, Rauscher SA, Seager R, Grissino-Mayer HD (2012) Temperature
6
7 766 as a potent driver of regional forest drought stress and tree mortality. *Nature*
8
9 767 *Clim Change* 3:292-297.
10
11
12 768
13
14 769
15
16 770
17
18 771
19
20
21 772
22
23
24 773
25
26
27 774
28
29
30 775
31
32
33 776
34
35
36 777
37
38 778
39
40 779
41
42
43 780
44
45
46 781
47
48
49 782
50
51 783
52
53
54 784
55
56 785
57
58
59
60

For Peer Review

786 **Figure legends**

787 Figure 1. Seasonal course of daily precipitation, soil water content (SWC), vapor
788 pressure deficit (VPD) and temperature during the study period. Error bars indicate ± 1
789 SE. Arrows in the upper panel indicate sampling days (carbohydrates sampling: solid
790 arrow; carbohydrates + embolism sampling: dotted arrow; embolism sampling: dashed
791 arrow).

792 Figure 2. Seasonal variation of total non-structural carbohydrates (TNSC) and the ratio
793 between soluble sugars and total non-structural carbohydrates (SS:TNSC) in the four
794 studied organs. Error bars indicate ± 1 SE. The asterisks indicate significant differences
795 between defoliation classes within a given sampling month (\bullet $0.05 < P < 0.1$; *
796 $0.01 < P < 0.05$; ** $0.001 < P < 0.01$; *** $P < 0.001$).

797 Figure 3. Seasonal changes in root starch concentration as a function of infection and
798 defoliation classes. Error bars indicate ± 1 SE.

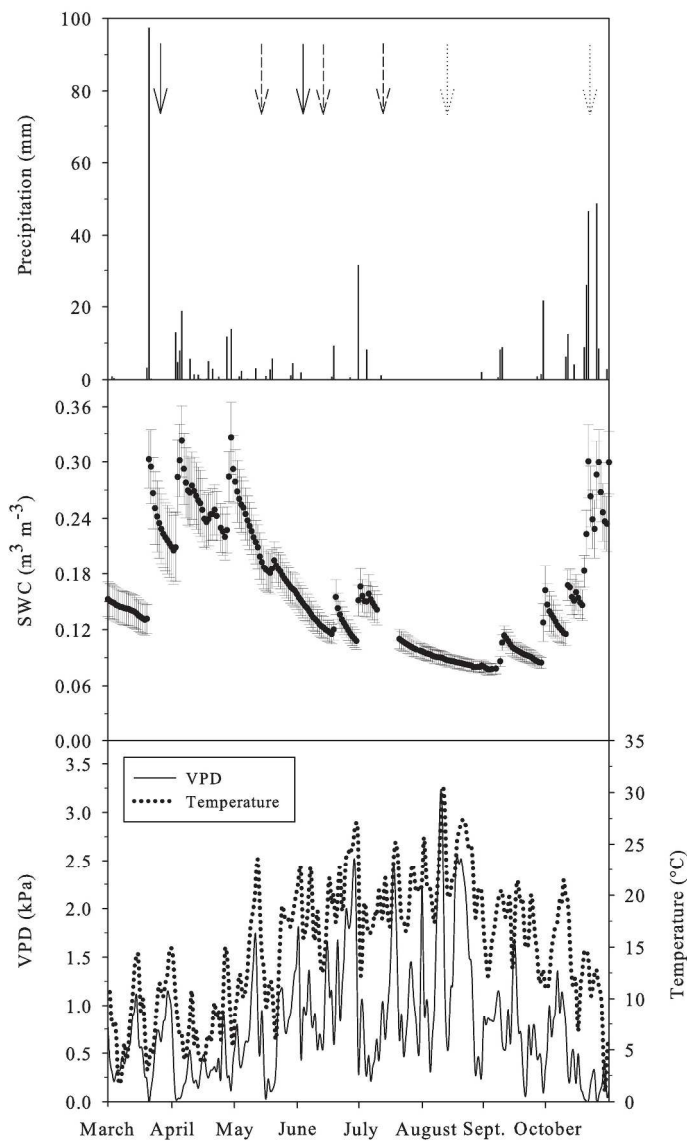
799 Figure 4. Vulnerability curves for roots (a) and branches (b) of defoliated and non-
800 defoliated Scots pine trees, showing percentage loss of hydraulic conductivity (PLC) as
801 a function of applied pressure. Equation 1 was used to fit the curves. Error bars indicate
802 ± 1 SE.

803 Figure 5. Seasonal variation of (a) native embolism expressed as percentage loss of
804 hydraulic conductivity (PLC) and (b) corresponding water potential, measured in the
805 same branches, of defoliated and non-defoliated Scots pine trees. Panel (c) shows
806 predawn and midday water potentials from nearby Scots pine trees from the same
807 population measured on the same dates, where solid lines and symbols indicate
808 defoliated trees and dashed lines and open symbols designate non-defoliated individuals.

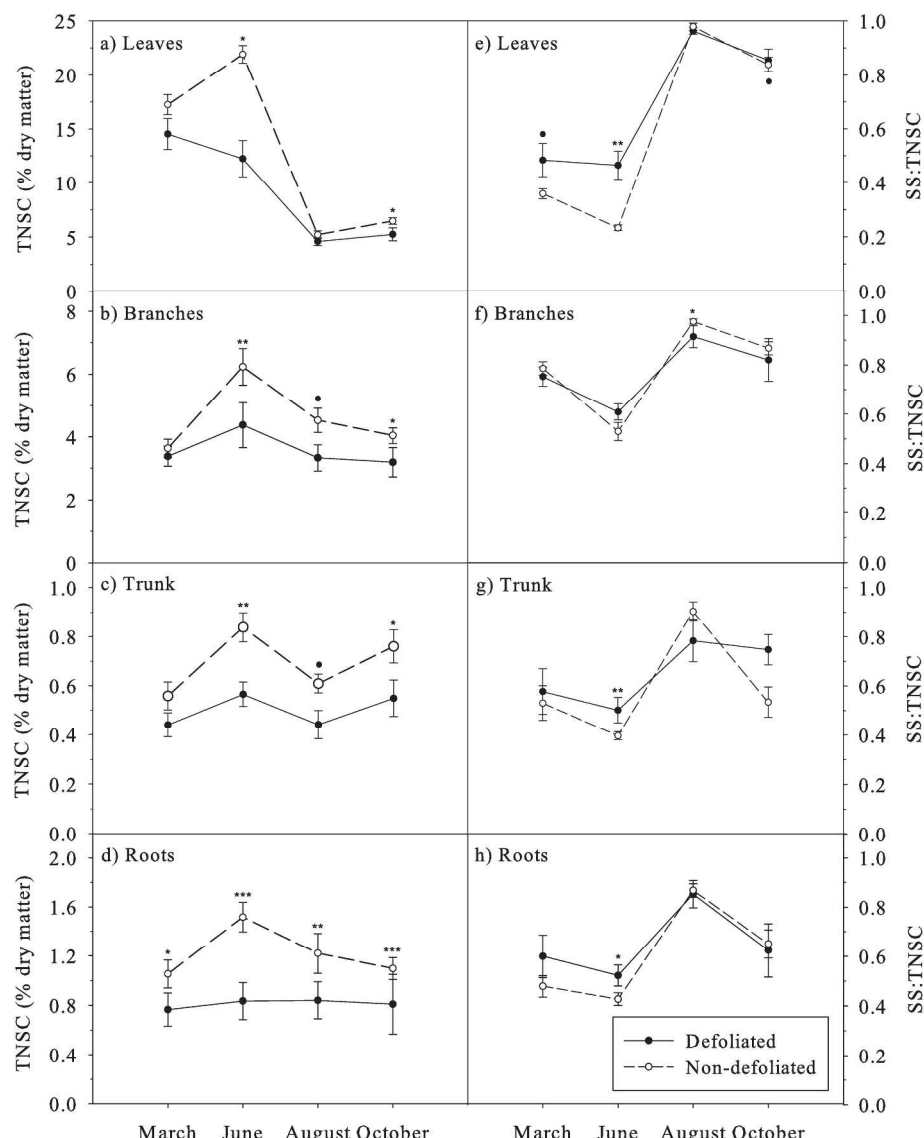
1
2
3 809 Error bars indicate ± 1 SE. Different letters indicate significant differences ($P<0.05$)
4
5 810 between sampling dates.
6
7

8 811 Figure 6. Basal area increment (BAI) (a), trunk sapwood depth (b), and root sapwood
9 depth (c) as a function of infection and defoliation classes. Different uppercase letters
10 indicate significant differences ($P<0.05$) between infestation occurrence, and different
11 lowercase letters indicate significant differences between defoliation classes within a
12 given infection class. Note that the interaction between defoliation and infection in the
13 BAI model was marginally significant ($0.05<P<0.1$). Error bars ± 1 SE.
14
15
16
17
18
19
20
21

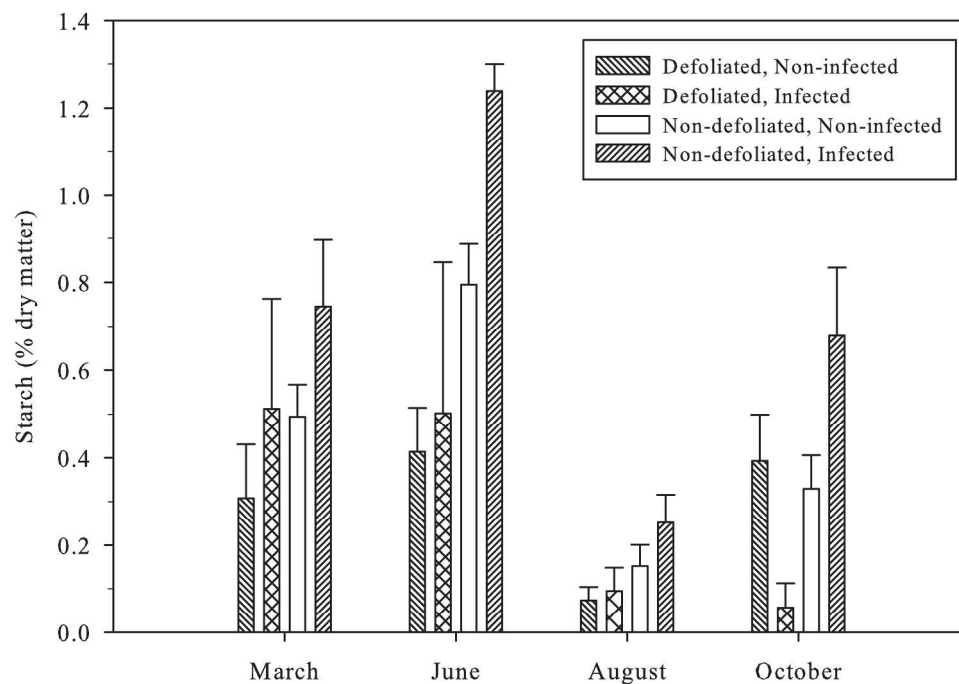
22 817 Figure 7. Schematic diagram of the processes associated with drought-induced mortality
23 in Scots pine at our study site in Prades. Different numbers depict studies where the
24 relationship has been reported: 1) Vilà-Cabrera et al. 2013, Poyatos et al. 2013, 2)
25 Poyatos et al. 2013, 3) Poyatos et al. 2013, 4) Heres et al. 2013, 5) Heres et al. 2012 and
26 6) Galiano et al. 2011. Only Galiano et al. 2011 refers to a study conducted in a nearby
27 population. Arrows indicate relationship between mechanisms. Dashed lines depict the
28 relationships examined in this study. Question marks identify consequences for which
29 the evidence is still weak. Letters inside “Tree NSC storage” compartment indicate
30 different levels of NSC: A) high levels (tree survives), B) medium levels (tree survives),
31 and C) low levels (tree dies).
32
33
34
35
36
37
38
39
40
41
42
43
44
45
46
47
48
49
50
51
52
53
54
55
56
57
58
59
60



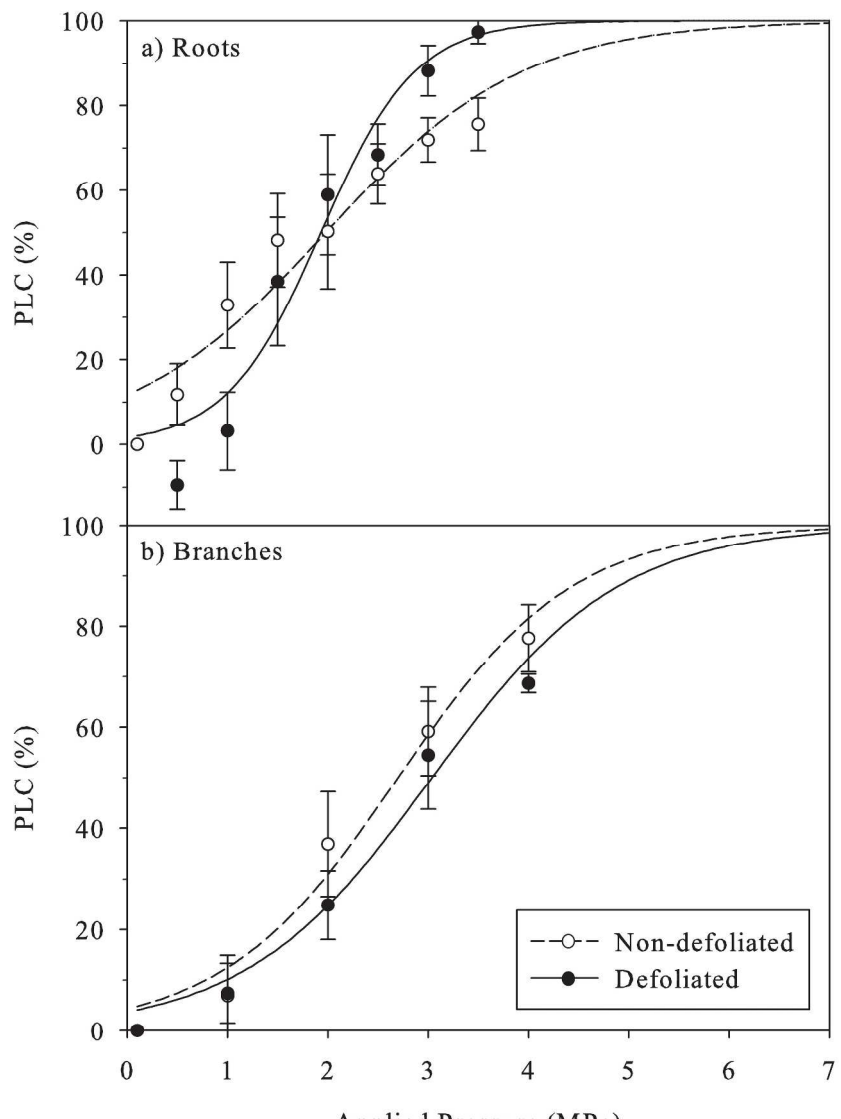
233x406mm (300 x 300 DPI)



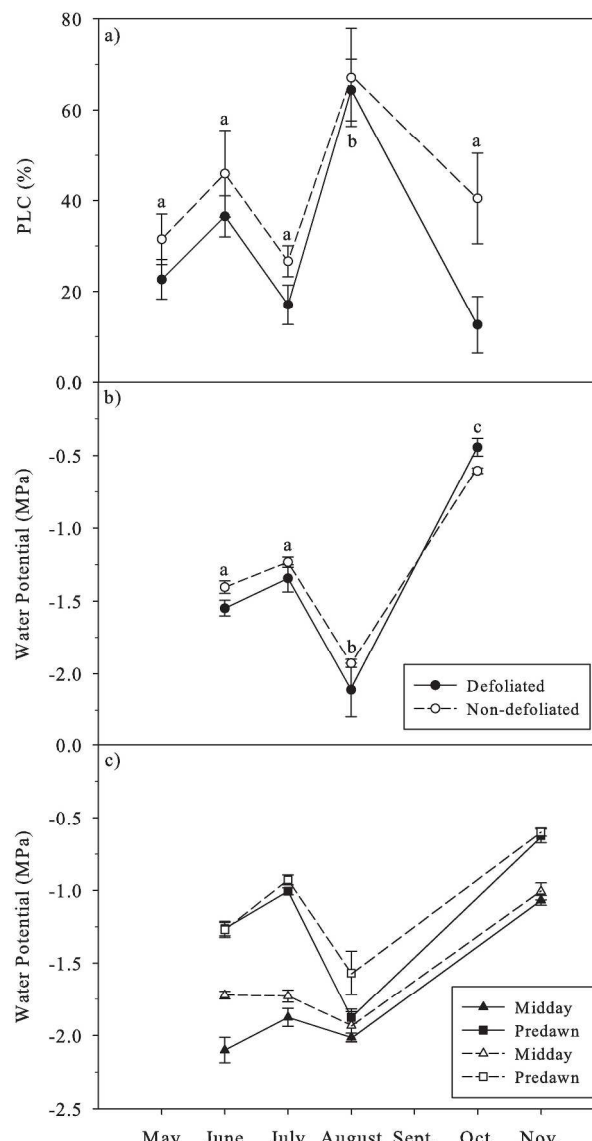
233x303mm (300 x 300 DPI)



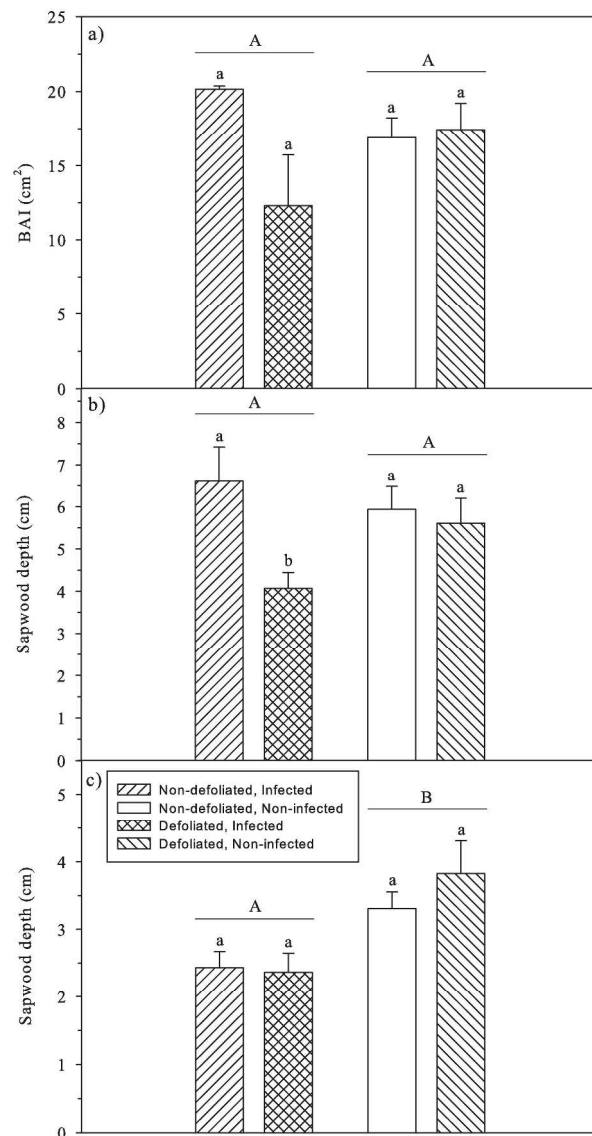
233x176mm (300 x 300 DPI)



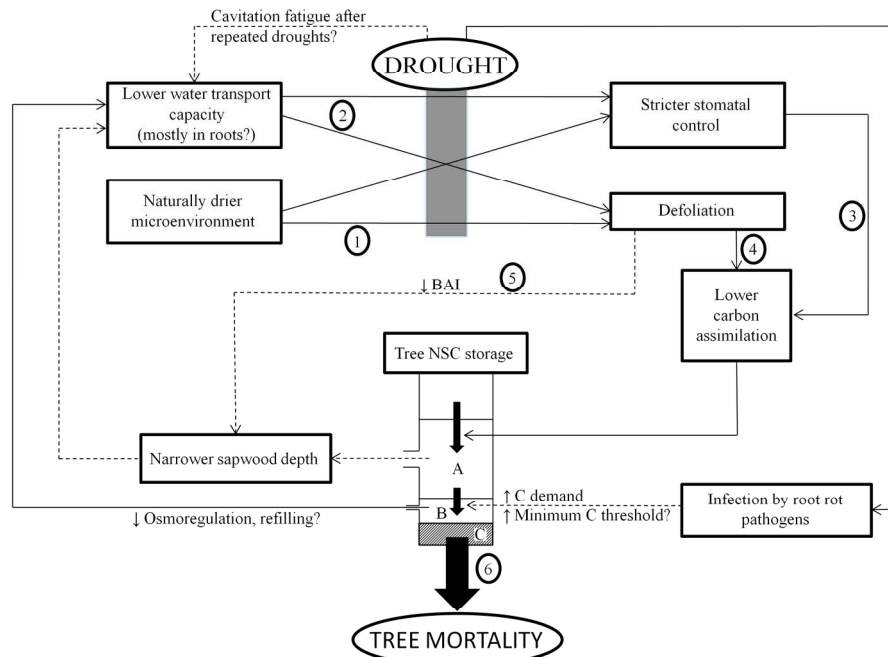
233x323mm (300 x 300 DPI)



233x449mm (300 x 300 DPI)



233x453mm (300 x 300 DPI)



190x142mm (300 x 300 DPI)

Tables

Table 1. Summary of the fitted linear mixed models with total non-structural carbohydrates (TNSC), the ratio between soluble sugars and total non-structural carbohydrates (SS:TNSC) and root starch as response variables. For factors, the coefficients indicate the difference between each level of a given variable and its reference level. In models the reference organ was “Leaves” (except in root starch where the effect of organ is not evaluated in the model), the reference month was “March”, the reference defoliation class was “Defoliated” and the reference infestation occurrence was “Infected”. The values are the estimate \pm SE. Abbreviations: (ns) = no significant differences; \cdot $0.05 < P < 0.1$; * $0.01 < P < 0.05$; ** $0.001 < P < 0.01$; *** $P < 0.001$; ne = not evaluated in the model. Conditional R^2 values are given for each model.

Parameter	log(TNSC)	SS:TNSC	sqrt(Starch)
	$R^2 = 0.90$	$R^2 = 0.61$	$R^2 = 0.57$
Intercept	$2.50 \pm 0.19^{***}$	$0.54 \pm 0.06^{***}$	$0.65 \pm 0.13^{***}$
Branches	$-1.31 \pm 0.19^{***}$	$0.27 \pm 0.07^{***}$	ne
Trunk	$-3.22 \pm 0.19^{***}$	0.10 ± 0.07 (ns)	ne
Roots	$-2.78 \pm 0.19^{***}$	0.07 ± 0.07 (ns)	ne
June	-0.15 ± 0.19 (ns)	-0.08 ± 0.07 (ns)	-0.02 ± 0.18 (ns)
August	$-1.17 \pm 0.19^{***}$	$0.41 \pm 0.07^{***}$	-0.40 ± 0.18 *
October	$-1.28 \pm 0.19^{***}$	$0.37 \pm 0.07^{***}$	-0.51 ± 0.18 **
Non-defoliated	0.15 ± 0.17 (ns)	-0.10 ± 0.05 *	0.21 ± 0.21
Non-infected	0.18 ± 0.20 (ns)	-0.09 ± 0.06 (ns)	-0.17 ± 0.16 (ns)
Branches:June	0.31 ± 0.19 (ns)	-0.13 ± 0.07 *	ne
Trunk:June	0.31 ± 0.19 (ns)	-0.03 ± 0.07 (ns)	ne
Roots:June	0.21 ± 0.19 (ns)	0.01 ± 0.07 (ns)	ne

1	Branches:August	1.23 ± 0.19***	-0.37 ± 0.08***	ne
2	Trunk:August	1.21 ± 0.19***	-0.26 ± 0.08***	ne
3	Roots:August	1.26 ± 0.19***	-0.23 ± 0.08**	ne
4	Branches:October	0.88 ± 0.19***	-0.35 ± 0.08***	ne
5	Trunk:October	1.26 ± 0.19***	-0.33 ± 0.08***	ne
6	Roots:October	0.90 ± 0.19***	-0.33 ± 0.08***	ne
7	Branches:Non-defoliated	0.05 ± 0.14 (ns)	0.10 ± 0.05*	ne
8	Trunk:Non-defoliated	0.05 ± 0.14 (ns)	0.02 ± 0.05 (ns)	ne
9	Roots:Non-defoliated	0.29 ± 0.14*	0.04 ± 0.05 (ns)	ne
10	Branches:Non-infected	-0.28 ± 0.16*	0.04 ± 0.06 (ns)	ne
11	Trunk:Non-infected	-0.36 ± 0.16*	0.03 ± 0.06 (ns)	ne
12	Roots:Non-infected	-0.39 ± 0.16*	0.03 ± 0.06 (ns)	ne
13	June:Non-defoliated	0.31 ± 0.14*	-0.07 ± 0.05 (ns)	0.28 ± 0.29 (ns)
14	August:Non-defoliated	0.14 ± 0.14 (ns)	0.11 ± 0.05*	0.04 ± 0.29 (ns)
15	October:Non-defoliated	0.27 ± 0.14 (ns)	0.01 ± 0.05 (ns)	0.47 ± 0.29 (ns)
16	June:Non-infected	0.04 ± 0.16 (ns)	0.05 ± 0.06 (ns)	0.15 ± 0.22 (ns)
17	August:Non-infected	-0.10 ± 0.16*	0.12 ± 0.06*	0.14 ± 0.22 (ns)
18	October:Non-infected	0.16 ± 0.16 (ns)	0.07 ± 0.06 (ns)	0.59 ± 0.22**
19	Non-defoliated:Non-infected	ne	ne	0 ± 0.24 (ns)
20	June:Non-defoliated:Non-infected	ne	ne	-0.22 ± 0.33 (ns)
21	August:Non-defoliated:Non-infected	ne	ne	-0.13 ± 0.33 (ns)
22	October:Non-defoliated:Non-infected	ne	ne	-0.72 ± 0.33*

1
2
3
4
5 Table 2. Summary of the fitted models with the vulnerability-curves parameters (a and P_{50}), specific hydraulic conductivity (K_S), leaf specific
6 conductivity (K_L) and leaf-to-sapwood area ratio ($A_L:As$) as response variables. In the models the reference organ was “Branches”, the reference
7
8 defoliation class was “Defoliated” and the infestation occurrence was “Infected”. The values are the estimate \pm SE. Abbreviations: (ns) = no
9 significant differences; $^* 0.05 < P < 0.1$; $^* 0.01 < P < 0.05$; $^{***} P < 0.001$; ne = not evaluated in the model. Conditional R^2 values are given for
10
11 each model.
12
13
14

Parameter	Parameter a	P_{50}	$\log(K_S)$	$\log(K_L)$	$\log(A_L:As)$
	$R^2 = 0.37$	$R^2 = 0.40$	$R^2 = 0.10$	$R^2 = 0.36$	$R^2 = 0.11$
Intercept	-2.04 ± 1.38 (ns)	$2.72 \pm 0.42^{***}$	$-8.70 \pm 0.81^{***}$	$-16.56 \pm 0.75^{***}$	$7.48 \pm 0.64^{***}$
Roots	-1.80 ± 1.78 (ns)	-0.99 ± 0.55 (ns)	0.20 ± 1.04 (ns)	ne	ne
Non-defoliated	-0.12 ± 1.20 (ns)	-0.51 ± 0.37 (ns)	0.01 ± 0.70 (ns)	1.90 ± 1.30 (ns)	-0.73 ± 1.10 (ns)
Non-infected	0.36 ± 1.50 (ns)	0.41 ± 0.46 (ns)	1.12 ± 0.88 (ns)	$2.50 \pm 0.89^*$	-0.83 ± 0.75 (ns)
Roots:Non-defoliated	$4.26 \pm 1.74^*$	0.42 ± 0.54 (ns)	0.16 ± 1.02 (ns)	ne	ne
Roots:Non-infected	-2.74 ± 1.99 (ns)	-0.12 ± 0.61 (ns)	-0.67 ± 1.16 (ns)	ne	ne
Non-defoliated:Non-infected	ne	ne	ne	$-2.71 \pm 1.44^*$	1.29 ± 1.22 (ns)

6

1

1
2
3 Table 3. Summary of the fitted linear mixed models with the percentage loss of conductivity
4
5 (PLC) and the water potential as response variables. The reference month was “May” in PLC
6
7 and “June” in Water Potential, the reference defoliation class was “Defoliated” and the
8
9 infestation occurrence was “Infected”. The values are the estimate \pm SE. Abbreviations: (ns)
10
11 = no significant differences; $^{\circ} 0.05 < P < 0.1$; $*$ $0.01 < P < 0.05$; $^{**} 0.001 < P < 0.01$; $^{***} P <$
12
13 0.001; ne = not evaluated in the model. Conditional R^2 values are given for each model.
14
15

Parameter	PLC	Water Potential
	R2 = 0.45	R2 = 0.82
Intercept	$23.01 \pm 10.98^*$	$-1.57 \pm 0.13^{***}$
June	10.95 ± 14.96 (ns)	ne
July	-9.95 ± 14.96 (ns)	-0.04 ± 0.19 (ns)
August	$45.23 \pm 14.96^{**}$	$-0.69 \pm 0.19^{***}$
October	-12.74 ± 15.00 (ns)	$1.14 \pm 0.19^{***}$
Non-defoliated	8.60 ± 10.47 (ns)	0.14 ± 0.13 (ns)
Non-infected	-0.52 ± 11.87 (ns)	0.02 ± 0.15 (ns)
June:Non-defoliated	0.25 ± 14.33 (ns)	ne
July:Non-defoliated	0.19 ± 14.33 (ns)	-0.07 ± 0.18 (ns)
August:Non-defoliated	-5.15 ± 14.33 (ns)	0.01 ± 0.18 (ns)
October:Non-defoliated	14.72 ± 14.64 (ns)	-0.30 ± 0.19 (ns)
June:Non-infected	4.42 ± 16.23 (ns)	ne
July:Non-infected	6.51 ± 16.23 (ns)	$0.37 \pm 0.21^{\circ}$
August:Non-infected	-5.16 ± 16.23 (ns)	0.20 ± 0.21 (ns)
October:Non-infected	9.13 ± 16.38 (ns)	-0.05 ± 0.21 (ns)